

CONSTRAINTS ON THE ORIGIN OF COSMIC RAYS ABOVE 10^{18} eV FROM LARGE-SCALE ANISOTROPY SEARCHES IN DATA OF THE PIERRE AUGER OBSERVATORY

THE PIERRE AUGER COLLABORATION⁹⁵,

P. ABREU¹, M. AGLIETTA², M. AHLERS³, E. J. AHN⁴, I. F. M. ALBUQUERQUE⁵, D. ALLARD⁶, I. ALLEKOTTE⁷, J. ALLEN⁸,
P. ALLISON⁹, A. ALMELA^{10,11}, J. ALVAREZ CASTILLO¹², J. ALVAREZ-MUÑOZ¹³, R. ALVES BATISTA¹⁴, M. AMBROSIO¹⁵,
A. AMINAEI¹⁶, L. ANCHORDOQUI¹⁷, S. ANDRINGA¹, T. ANTIČIĆ¹⁸, C. ARAMO¹⁵, E. ARGANDA^{19,20}, F. ARQUEROS²⁰, H. ASOREY⁷,
P. ASSIS¹, J. AUBLIN²¹, M. AVE²², M. AVENIER²³, G. AVILA²⁴, A. M. BADESCU²⁵, M. BALZER²⁶, K. B. BARBER²⁷,
A. F. BARBOSA^{28,96}, R. BARDENET²⁹, S. L. C. BARROSO³⁰, B. BAUGHMAN^{9,97}, J. BÄUML³¹, C. BAUS²², J. J. BEATTY⁹,
K. H. BECKER³², A. BELLÉTOILE³³, J. A. BELLIDO²⁷, S. BENZVI³, C. BERAT²³, X. BERTOU⁷, P. L. BIERMANN³⁴,
P. BILLOIR²¹, F. BLANCO²⁰, M. BLANCO^{21,35}, C. BLEVE³², H. BLÜMER^{22,31}, M. BOHÁČOVÁ³⁶, D. BONCIOLI³⁷,
C. BONIFAZI^{21,38}, R. BONINO², N. BORODAI³⁹, J. BRACK⁴⁰, I. BRANCUS⁴¹, P. BROGUEIRA¹, W. C. BROWN⁴², R. BRUIJN^{43,98},
P. BUCHHOLZ⁴⁴, A. BUENO⁴⁵, L. BUROKER¹⁷, R. E. BURTON⁴⁶, K. S. CABALLERO-MORA⁴⁷, B. CACCIANIGA⁴⁸, L. CARAMETE³⁴,
R. CARUSO⁴⁹, A. CASTELLINA², O. CATALANO⁵⁰, G. CATALDI⁵¹, L. CAZON¹, R. CESTER⁵², J. CHAUVIN²³, S. H. CHENG⁴⁷,
A. CHIAVASSA², J. A. CHINELLATO¹⁴, J. CHIRINOS DIAZ⁵³, J. CHUDOBA³⁶, M. CILMO¹⁵, R. W. CLAY²⁷, G. COCCIOLLO⁵¹,
L. COLLICA⁴⁸, M. R. COLUCCIA⁵¹, R. CONCEIÇÃO¹, F. CONTRERAS⁵⁴, H. COOK⁴³, M. J. COOPER²⁷, J. COPPENS^{16,55}, A. CORDIER²⁹,
S. COUTU⁴⁷, C. E. COVAULT⁴⁶, A. CREUSOT⁶, A. CRISS⁴⁷, J. CRONIN⁵⁶, A. CURUTIU³⁴, S. DAGORET-CAMPAGNE²⁹, R. DALLIER³³,
B. DANIEL¹⁴, S. DASSO^{57,58}, K. DAUMILLER³¹, B. R. DAWSON²⁷, R. M. DE ALMEIDA⁵⁹, M. DE DOMENICO⁴⁹, C. DE DONATO¹²,
S. J. DE JONG^{16,55}, G. DE LA VEGA⁶⁰, W. J. M. DE MELLO JUNIOR¹⁴, J. R. T. DE MELLO NETO³⁸, I. DE MITRI⁵¹, V. DE SOUZA⁶¹,
K. D. DE VRIES⁶², L. DEL PERAL³⁵, M. DEL RÍO^{37,54}, O. DELIGNY⁶³, H. DEMBINSKI²², N. DHITAL⁵³, C. DI GIULIO^{37,64},
M. L. DÍAZ CASTRO²⁸, P. N. DIEP⁶⁵, F. DIOGO¹, C. DOBRIGKEIT¹⁴, W. DOCTERS⁶², J. C. D'OLIVO¹², P. N. DONG^{63,65},
A. DOROFEEV⁴⁰, J. C. DOS ANJOS²⁸, M. T. DOVA¹⁹, D. D'URSO¹⁵, I. DUTAN³⁴, J. EBR³⁶, R. ENGEL³¹, M. ERDMANN⁶⁶,
C. O. ESCOBAR^{4,14}, J. ESPADANAL¹, A. ETCHEGOYEN^{10,11}, P. FACAL SAN LUIS⁵⁶, H. FALCKE^{16,55,67}, K. FANG⁵⁶, G. FARRAR⁸,
A. C. FAUTH¹⁴, N. FAZZINI⁴, A. P. FERGUSON⁴⁶, B. FICK⁵³, J. M. FIGUEIRA¹¹, A. FILEVICH¹¹, A. FILIPČIĆ^{68,69}, S. FLIESCHER⁶⁶,
C. E. FRACCHIOLLA⁴⁰, E. D. FRAENKEL⁶², O. FRATU²⁵, U. FRÖHLICH⁴⁴, B. FUCHS²², R. GAIOR²¹, R. F. GAMARRA¹¹, S. GAMBETTA⁷⁰,
B. GARCÍA⁶⁰, S. T. GARCIA ROCA¹³, D. GARCIA-GAMEZ²⁹, D. GARCIA-PINTO²⁰, G. GARILLI⁴⁹, A. GASCON BRAVO⁴⁵, H. GEMMEKE²⁶,
P. L. GHIA²¹, M. GILLER⁷¹, J. GITTO⁶⁰, H. GLASS⁴, M. S. GOLD⁷², G. GOLUP⁷, F. GOMEZ ALBARRACIN¹⁹, M. GÓMEZ BERISSO⁷,
P. F. GÓMEZ VITALE²⁴, P. GONÇALVES¹, J. G. GONZALEZ³¹, B. GOOKIN⁴⁰, A. GORGI², P. GOUFFON⁵, E. GRASHORN⁹, S. GREBE^{16,55},
N. GRIFFITH⁹, A. F. GRILLO⁷³, Y. GUARDINCERRI⁵⁸, F. GUARINO¹⁵, G. P. GUEDES⁷⁴, P. HANSEN¹⁹, D. HARARI⁷, T. A. HARRISON²⁷,
J. L. HARTON⁴⁰, A. HAUNGS³¹, T. HEBBEKER⁶⁶, D. HECK³¹, A. E. HERVE²⁷, G. C. HILL²⁷, C. HOJVAT⁴, N. HOLLON⁵⁶,
V. C. HOLMES²⁷, P. HOMOLA³⁹, J. R. HÖRANDEL^{16,55}, P. HORVATH⁷⁵, M. HRABOVSKÝ^{36,75}, D. HUBER²², T. HUEGE³¹, A. INSOLIA⁴⁹,
F. IONITA⁵⁶, A. ITALIANO⁴⁹, S. JANSEN^{16,55}, C. JARNE¹⁹, S. JIRASKOVA¹⁶, M. JOSEBACHUILI¹¹, K. KADIJA¹⁸, K. H. KAMPERT³²,
P. KARHAN⁷⁶, P. KASPER⁴, I. KATKOV²², B. KÉGL²⁹, B. KEILHAUER³¹, A. KEIVANI⁷⁷, J. L. KELLEY¹⁶, E. KEMP¹⁴,
R. M. KIECKHAFER⁵³, H. O. KLAGES³¹, M. KLEIFGES²⁶, J. KLEINFELLER^{31,54}, J. KNAPP⁴³, D.-H. KOANG²³, K. KOTERA⁵⁶,
N. KROHM³², O. KRÖMER²⁶, D. KRUPPKE-HANSEN³², D. KUEMPEL^{44,66}, J. K. KULBARTZ⁷⁸, N. KUNKA²⁶, G. LA ROSA⁵⁰,
C. LACHAUD⁶, D. LAHURD⁴⁶, L. LATRONICO², R. LAUER⁷², P. LAUTRIDOU³³, S. LE COZ²³, M. S. A. B. LEÃO⁷⁹, D. LEBRUN²³,
P. LEBRUN⁴, M. A. LEIGUI DE OLIVEIRA⁷⁹, A. LETESSIER-SELVON²¹, I. LHENRY-YVON⁶³, K. LINK²², R. LÓPEZ⁸⁰,
A. LOPEZ AGÜERA¹³, K. LOUEDEC^{23,29}, J. LOZANO BAHILLO⁴⁵, L. LU⁴³, A. LUCERO¹¹, M. LUDWIG²², H. LYBERIS^{38,63},
M. C. MACCARONE⁵⁰, C. MACOLINO²¹, S. MALDERA², J. MALLER³³, D. MANDAT³⁶, P. MANTSCH⁴, A. G. MARIAZZI¹⁹, J. MARIN^{2,54},
V. MARIN³³, I. C. MARIS²¹, H. R. MARQUEZ FALCON⁸¹, G. MARSELLA⁵¹, D. MARTELLO⁵¹, L. MARTIN³³, H. MARTINEZ⁸²,
O. MARTÍNEZ BRAVO⁸⁰, D. MARTRAIRE⁶³, J. J. MASÍAS MEZA⁵⁸, H. J. MATHES³¹, J. MATTHEWS⁷⁷, J. A. J. MATTHEWS⁷²,
G. MATTHIAE³⁷, D. MAUREL³¹, D. MAURIZIO^{28,52}, P. O. MAZUR⁴, G. MEDINA-TANCO¹², M. MELISSAS²², D. MELO¹¹,
E. MENICETTI⁵², A. MENSNIKOV²⁶, P. MERTSCH⁸³, S. MESSINA⁶², C. MEURER⁶⁶, R. MEYHANDAN⁸⁴, S. MIĆCANOVIĆ¹⁸,
M. I. MICHELETTI⁸⁵, I. A. MINAYA²⁰, L. MIRAMONTI⁴⁸, L. MOLINA-BUENO⁴⁵, S. MOLLERACH⁷, M. MONASOR⁵⁶,
D. MONNIER RAGAIGNE²⁹, F. MONTANET²³, B. MORALES¹², C. MORELLO², E. MORENO⁸⁰, J. C. MORENO¹⁹, M. MOSTAFÁ⁴⁰,
C. A. MOURA⁷⁹, M. A. MULLER¹⁴, G. MÜLLER⁶⁶, M. MÜNCHMEYER²¹, R. MUSSA⁵², G. NAVARRA^{2,96}, J. L. NAVARRO⁴⁵, S. NAVAS⁴⁵,
P. NECESAL³⁶, L. NELLEN¹², A. NELLES^{16,55}, J. NEUSER³², P. T. NHUNG⁶⁵, M. NIECHCIOL⁴⁴, L. NIEMIETZ³², N. NIERSTENHOEFER³²,
D. NITZ⁵³, D. NOSEK⁷⁶, L. NOŽKA³⁶, J. OEHLISCHLÄGER³¹, A. OLINTO⁵⁶, M. ORTIZ²⁰, N. PACHECO³⁵, D. PAKK SELMI-DEI¹⁴,
M. PALATKA³⁶, J. PALLOTTA⁸⁶, N. PALMIERI²², G. PARENTE¹³, E. PARIZOT⁶, A. PARRA¹³, S. PASTOR⁸⁷, T. PAUL⁸⁸, M. PECH³⁶,
J. PEKALA³⁹, R. PELAYO^{13,80}, I. M. PEPE⁸⁹, L. PERRONE⁵¹, R. PESCE⁷⁰, E. PETERMANN⁹⁰, S. PETRERA⁶⁴, A. PETROLINI⁷⁰,
Y. PETROV⁴⁰, C. PFENDNER³, R. PIEGAIA⁵⁸, T. PIEROG³¹, P. PIERONI⁵⁸, M. PIMENTA¹, V. PIRRONELLO⁴⁹, M. PLATINO¹¹, M. PLUM⁶⁶,
V. H. PONCE⁷, M. PONTZ⁴⁴, A. PORCELLI³¹, P. PRIVITERA⁵⁶, M. PROUZA³⁶, E. J. QUEL⁸⁶, S. QUERCHFELD³², J. RAUTENBERG³²,
O. RAVEL³³, D. RAVIGNANI¹¹, B. REVENU³³, J. RIDKY³⁶, S. RIGGI¹³, M. RISSE⁴⁴, P. RISTORI⁸⁶, H. RIVERA⁴⁸, V. RIZI⁶⁴, J. ROBERTS⁸,
W. RODRIGUES DE CARVALHO¹³, G. RODRIGUEZ¹³, I. RODRIGUEZ CABO¹³, J. RODRIGUEZ MARTINO⁵⁴, J. RODRIGUEZ ROJO⁵⁴,
M. D. RODRÍGUEZ-FRÍAS³⁵, G. ROS³⁵, J. ROSADO²⁰, T. ROSSLER⁷⁵, M. ROTH³¹, B. ROUILLÉ-D'ORFEUIL⁵⁶, E. ROULET⁷,
A. C. ROVERO⁵⁷, C. RÜHLE²⁶, A. SAFTIOU⁴¹, F. SALAMIDA⁶³, H. SALAZAR⁸⁰, F. SALESA GREUS⁴⁰, G. SALINA³⁷, F. SÁNCHEZ¹¹,
C. E. SANTO¹, E. SANTOS¹, E. M. SANTOS³⁸, F. SARAZIN⁹¹, B. SARKAR³², S. SARKAR⁸³, R. SATO⁵⁴, N. SCHARF⁶⁶, V. SCHERINI⁴⁸,

H. SCHIELER³¹, P. SCHIFFER^{66,78}, A. SCHMIDT²⁶, O. SCHOLTEN⁶², H. SCHOORLEMMER^{16,55}, J. SCHOVANCOVA³⁶, P. SCHOVÁNEK³⁶, F. SCHRÖDER³¹, D. SCHUSTER⁹¹, S. J. SCIUTTO¹⁹, M. SCUDERI⁴⁹, A. SEGRETO⁵⁰, M. SETTIMO⁴⁴, A. SHADKAM⁷⁷, R. C. SHELLARD²⁸, I. SIDELNIK¹¹, G. SIGL⁷⁸, H. H. SILVA LOPEZ¹², O. SIMA⁹², A. ŚMIAŁKOWSKI⁷¹, R. ŠMÍDA³¹, G. R. SNOW⁹⁰, P. SOMMERS⁴⁷, J. SOROKIN²⁷, H. SPINKA^{4,93}, R. SQUARTINI⁵⁴, Y. N. SRIVASTAVA⁸⁸, S. STANIC⁶⁹, J. STAPLETON⁹, J. STASIELAK³⁹, M. STEPHAN⁶⁶, A. STUTZ²³, F. SUAREZ¹¹, T. SUOMIJÄRVI⁶³, A. D. SUPANITSKY⁵⁷, T. ŠUŠA¹⁸, M. S. SUTHERLAND⁷⁷, J. SWAIN⁸⁸, Z. SZADKOWSKI⁷¹, M. SZUBA³¹, A. TAPIA¹¹, M. TARTARE²³, O. TAŞÇAU³², R. TCACIUC⁴⁴, N. T. THAO⁶⁵, D. THOMAS⁴⁰, J. TIFFENBERG⁵⁸, C. TIMMERMANS^{16,55}, W. TKACZYK^{71,96}, C. J. TODERO PEIXOTO⁶¹, G. TOMA⁴¹, L. TOMANKOVA³⁶, B. TOMÉ¹, A. TONACHINI⁵², G. TORRALBA ELIPE¹³, P. TRAVNICEK³⁶, D. B. TRIDAPALLI⁵, G. TRISTRAM⁶, E. TROVATO⁴⁹, M. TUEROS¹³, R. ULRICH³¹, M. UNGER³¹, M. URBAN²⁹, J. F. VALDÉS GALICIA¹², I. VALIÑO¹³, L. VALORE¹⁵, G. VAN AAR¹⁶, A. M. VAN DEN BERG⁶², S. VAN VELZEN¹⁶, A. VAN VLIET⁷⁸, E. VARELA⁸⁰, B. VARGAS CÁRDENAS¹², J. R. VÁZQUEZ²⁰, R. A. VÁZQUEZ¹³, D. VEBERIČ^{68,69}, V. VERZI³⁷, J. VICHA³⁶, M. VIDELA⁶⁰, L. VILLASEÑOR⁸¹, H. WAHLBERG¹⁹, P. WAHRLICH²⁷, O. WAINBERG^{10,11}, D. WALZ⁶⁶, A. A. WATSON⁴³, M. WEBER²⁶, K. WEIDENHAUPT⁶⁶, A. WEINDL³¹, F. WERNER³¹, S. WESTERHOFF³, B. J. WHELAN^{27,47}, A. WIDOM⁸⁸, G. WIECZOREK⁷¹, L. WIENCKE⁹¹, B. WILCZYŃSKA³⁹, H. WILCZYŃSKI³⁹, M. WILL³¹, C. WILLIAMS⁵⁶, T. WINCHEN⁶⁶, M. WOMMER³¹, B. WUNDHEILER¹¹, T. YAMAMOTO^{56,99}, T. YAPICI⁵³, P. YOUNK^{44,94}, G. YUAN⁷⁷, A. YUSHKOV¹³, B. ZAMORANO GARCIA⁴⁵, E. ZAS¹³, D. ZAVRTANIK^{68,69}, M. ZAVRTANIK^{68,69}, I. ZAW^{8,100}, A. ZEPEDA^{82,101}, J. ZHOU⁵⁶, Y. ZHU²⁶, M. ZIMBRES SILVA^{14,32}, AND M. ZIOLKOWSKI⁴⁴

¹ LIP and Instituto Superior Técnico, Technical University of Lisbon, Portugal

² Istituto di Fisica dello Spazio Interplanetario (INAF), Università di Torino and Sezione INFN, Torino, Italy

³ University of Wisconsin, Madison, WI, USA

⁴ Fermilab, Batavia, IL, USA

⁵ Universidade de São Paulo, Instituto de Física, São Paulo, SP, Brazil

⁶ Laboratoire AstroParticule et Cosmologie (APC), Université Paris 7, CNRS-IN2P3, Paris, France

⁷ Centro Atómico Bariloche and Instituto Balseiro (CNEA-UNCuyo-CONICET), San Carlos de Bariloche, Argentina

⁸ New York University, New York, NY, USA

⁹ Ohio State University, Columbus, OH, USA

¹⁰ Universidad Tecnológica Nacional - Facultad Regional Buenos Aires, Buenos Aires, Argentina

¹¹ Instituto de Tecnologías en Detección y Astropartículas (CNEA, CONICET, UNSAM), Buenos Aires, Argentina

¹² Universidad Nacional Autónoma de México, México, D.F., México

¹³ Universidad de Santiago de Compostela, Spain

¹⁴ Universidade Estadual de Campinas, IFGW, Campinas, SP, Brazil

¹⁵ Università di Napoli "Federico II" and Sezione INFN, Napoli, Italy

¹⁶ IMAPP, Radboud University Nijmegen, The Netherlands

¹⁷ University of Wisconsin, Milwaukee, WI, USA

¹⁸ Rudjer Bošković Institute, 10000 Zagreb, Croatia

¹⁹ IFLP, Universidad Nacional de La Plata and CONICET, La Plata, Argentina

²⁰ Universidad Complutense de Madrid, Madrid, Spain

²¹ Laboratoire de Physique Nucléaire et de Hautes Energies (LPNHE), Universités Paris 6 et Paris 7, CNRS-IN2P3, Paris, France

²² Karlsruhe Institute of Technology - Campus South - Institut für Experimentelle Kernphysik (IEKP), Karlsruhe, Germany

²³ Laboratoire de Physique Subatomique et de Cosmologie (LPSC), Université Joseph Fourier Grenoble, CNRS-IN2P3, Grenoble INP, France

²⁴ Observatorio Pierre Auger and Comisión Nacional de Energía Atómica, Malargüe, Argentina

²⁵ University Politehnica of Bucharest, Romania

²⁶ Karlsruhe Institute of Technology - Campus North - Institut für Prozessdatenverarbeitung und Elektronik, Karlsruhe, Germany

²⁷ University of Adelaide, Adelaide, S.A., Australia

²⁸ Centro Brasileiro de Pesquisas Físicas, Rio de Janeiro, RJ, Brazil

²⁹ Laboratoire de l'Accélérateur Linéaire (LAL), Université Paris 11, CNRS-IN2P3, France

³⁰ Universidade Estadual do Sudoeste da Bahia, Vitória da Conquista, BA, Brazil

³¹ Karlsruhe Institute of Technology - Campus North - Institut für Kernphysik, Karlsruhe, Germany

³² Bergische Universität Wuppertal, Wuppertal, Germany

³³ SUBATECH, École des Mines de Nantes, CNRS-IN2P3, Université de Nantes, France

³⁴ Max-Planck-Institut für Radioastronomie, Bonn, Germany

³⁵ Universidad de Alcalá, Alcalá de Henares (Madrid), Spain

³⁶ Institute of Physics of the Academy of Sciences of the Czech Republic, Prague, Czech Republic

³⁷ Università di Roma II "Tor Vergata" and Sezione INFN, Roma, Italy

³⁸ Universidade Federal do Rio de Janeiro, Instituto de Física, Rio de Janeiro, RJ, Brazil

³⁹ Institute of Nuclear Physics PAN, Krakow, Poland

⁴⁰ Colorado State University, Fort Collins, CO, USA

⁴¹ "Horia Hulubei" National Institute for Physics and Nuclear Engineering, Bucharest- Magurele, Romania

⁴² Colorado State University, Pueblo, CO, USA

⁴³ School of Physics and Astronomy, University of Leeds, UK

⁴⁴ Universität Siegen, Siegen, Germany

⁴⁵ Universidad de Granada & C.A.F.P.E., Granada, Spain

⁴⁶ Case Western Reserve University, Cleveland, OH, USA

⁴⁷ Pennsylvania State University, University Park, PA, USA

⁴⁸ Università di Milano and Sezione INFN, Milan, Italy

⁴⁹ Università di Catania and Sezione INFN, Catania, Italy

⁵⁰ Istituto di Astrofisica Spaziale e Fisica Cosmica di Palermo (INAF), Palermo, Italy

⁵¹ Dipartimento di Matematica e Fisica "E. De Giorgi" dell'Università del Salento and Sezione INFN, Lecce, Italy

⁵² Università di Torino and Sezione INFN, Torino, Italy

⁵³ Michigan Technological University, Houghton, MI, USA

- ⁵⁴ Observatorio Pierre Auger, Malargüe, Argentina
⁵⁵ Nikhef, Science Park, Amsterdam, The Netherlands
⁵⁶ University of Chicago, Enrico Fermi Institute, Chicago, IL, USA
⁵⁷ Instituto de Astronomía y Física del Espacio (CONICET-UBA), Buenos Aires, Argentina
⁵⁸ Departamento de Física, FCEyN, Universidad de Buenos Aires y CONICET, Argentina
⁵⁹ Universidade Federal Fluminense, EEIMVR, Volta Redonda, RJ, Brazil
⁶⁰ National Technological University, Faculty Mendoza (CONICET/CNEA), Mendoza, Argentina
⁶¹ Universidade de São Paulo, Instituto de Física, São Carlos, SP, Brazil
⁶² Kernfysisch Versneller Instituut, University of Groningen, Groningen, The Netherlands
⁶³ Institut de Physique Nucléaire d'Orsay (IPNO), Université Paris 11, CNRS-IN2P3, Orsay, France
⁶⁴ Università dell'Aquila and INFN, L'Aquila, Italy
⁶⁵ Institute for Nuclear Science and Technology (INST), Hanoi, Vietnam
⁶⁶ RWTH Aachen University, III. Physikalisches Institut A, Aachen, Germany
⁶⁷ ASTRON, Dwingeloo, The Netherlands
⁶⁸ J. Stefan Institute, Ljubljana, Slovenia
⁶⁹ Laboratory for Astroparticle Physics, University of Nova Gorica, Slovenia
⁷⁰ Dipartimento di Fisica dell'Università and INFN, Genova, Italy
⁷¹ University of Łódź, Łódź, Poland
⁷² University of New Mexico, Albuquerque, NM, USA
⁷³ INFN, Laboratori Nazionali del Gran Sasso, Assergi (L'Aquila), Italy
⁷⁴ Universidade Estadual de Feira de Santana, Brazil
⁷⁵ Palacky University, RCPTM, Olomouc, Czech Republic
⁷⁶ Charles University, Faculty of Mathematics and Physics, Institute of Particle and Nuclear Physics, Prague, Czech Republic
⁷⁷ Louisiana State University, Baton Rouge, LA, USA
⁷⁸ Universität Hamburg, Hamburg, Germany
⁷⁹ Universidade Federal do ABC, Santo André, SP, Brazil
⁸⁰ Benemérita Universidad Autónoma de Puebla, Puebla, Mexico
⁸¹ Universidad Michoacana de San Nicolas de Hidalgo, Morelia, Michoacan, Mexico
⁸² Centro de Investigación y de Estudios Avanzados del IPN (CINVESTAV), México, Mexico
⁸³ Rudolf Peierls Centre for Theoretical Physics, University of Oxford, Oxford, UK
⁸⁴ University of Hawaii, Honolulu, HI, USA
⁸⁵ Instituto de Física de Rosario (IFIR) - CONICET/U.N.R. and Facultad de Ciencias Bioquímicas y Farmacéuticas U.N.R., Rosario, Argentina
⁸⁶ Centro de Investigaciones en Láseres y Aplicaciones, CITEDEF and CONICET, Argentina
⁸⁷ Instituto de Física Corpuscular, CSIC-Universitat de València, Valencia, Spain
⁸⁸ Northeastern University, Boston, MA, USA
⁸⁹ Universidade Federal da Bahia, Salvador, BA, Brazil
⁹⁰ University of Nebraska, Lincoln, NE, USA
⁹¹ Colorado School of Mines, Golden, CO, USA
⁹² University of Bucharest, Physics Department, Romania
⁹³ Argonne National Laboratory, Argonne, IL, USA
⁹⁴ Los Alamos National Laboratory, Los Alamos, NM, USA

Received 2012 October 22; accepted 2012 November 25; published 2012 December 12

ABSTRACT

A thorough search for large-scale anisotropies in the distribution of arrival directions of cosmic rays detected above 10^{18} eV at the Pierre Auger Observatory is reported. For the first time, these large-scale anisotropy searches are performed as a function of both the right ascension and the declination and expressed in terms of dipole and quadrupole moments. Within the systematic uncertainties, no significant deviation from isotropy is revealed. Upper limits on dipole and quadrupole amplitudes are derived under the hypothesis that any cosmic ray anisotropy is dominated by such moments in this energy range. These upper limits provide constraints on the production of cosmic rays above 10^{18} eV, since they allow us to challenge an origin from stationary galactic sources densely distributed in the galactic disk and emitting predominantly light particles in all directions.

Key words: astroparticle physics – cosmic rays

Online-only material: color figures

The large-scale distribution of arrival directions of Ultra-High Energy Cosmic Rays (UHECRs) as a function of the energy is a key observable to provide further understanding of their origin. Above $\simeq 0.25$ EeV, the most stringent bounds ever obtained on the dipole component in the equatorial plane were recently reported, being below 2% at 99% CL for EeV energies (Pierre

Auger Collaboration 2011a). Such a sensitivity provides some constraints upon scenarios in which dipolar anisotropies could be imprinted in the distribution of arrival directions as the result of the escape of UHECRs from the Galaxy up to the ankle energy (Ptuskin et al. 1993; Candia et al. 2003; Giacinti et al. 2012). On the other hand, if UHECRs above 1 EeV already have a predominant extragalactic origin (Hillas 1967; Blumenthal 1970; Berezhinsky et al. 2006, 2004), their angular distribution is expected to be isotropic to a high level. Thus, the study of large-scale anisotropies at EeV energies would help in establishing whether the origin of UHECRs is galactic or extragalactic in this energy range.

The upper limits aforementioned are based on first harmonic analyses of the right ascension distributions in several energy

⁹⁵ Av. San Martín Norte 306, 5613 Malargüe, Mendoza, Argentina; www.auger.org.

⁹⁶ Deceased.

⁹⁷ Now at University of Maryland.

⁹⁸ Now at Université de Lausanne.

⁹⁹ At Konan University, Kobe, Japan.

¹⁰⁰ Now at NYU Abu Dhabi.

¹⁰¹ Now at the Universidad Autonoma de Chiapas on leave of absence from Cinvestav.

ranges. The analyses benefit from the almost uniform directional exposure in right ascension of any ground-based observatory operating with high duty cycle, but are not sensitive to a dipole component along the Earth rotation axis. In contrast, using the large amount of data collected by the surface detector array of the Pierre Auger Observatory, in this Letter we report on searches for dipole and quadrupole patterns significantly standing out above the background noise whose components are functions of *both* the right ascension and the declination (a detailed description of the present analysis can be found in Pierre Auger Collaboration 2012).

The Pierre Auger Observatory is located in Malargüe, Argentina, at a mean latitude of $35^{\circ}2$ S, a mean longitude of $69^{\circ}5$ W, and a mean altitude of 1400 m above sea level. It exploits two available techniques to detect extensive air showers initiated by UHECRs: a surface detector (SD) array and a fluorescence detector (FD). The SD array consists of 1660 water-Cherenkov detectors laid out over about 3000 km² on a triangular grid with 1.5 km spacing, sensitive to the light emitted in their volume by the secondary particles of the showers. At the perimeter of this array, the atmosphere is overlooked on dark nights by 27 optical telescopes grouped in 5 buildings. These telescopes record the number of secondary charged particles in the air shower as a function of depth in the atmosphere by measuring the amount of nitrogen fluorescence caused by those particles along the track of the shower. At the lowest energies observed, the angular resolution of the SD is about $2^{\circ}2$ and reaches $\sim 1^{\circ}$ at the highest energies. This is sufficient to perform searches for large-scale anisotropies. The statistical fluctuation in energy measurement amounts to about 15%, while the absolute energy scale is given by the FD measurements and has a systematic uncertainty of 22% (Pierre Auger Collaboration 2008).

In the analyses presented in this Letter, the data set consists of events recorded by the SD array from 2004 January 1 to 2011 December 31, with zenith angles less than 55° . To ensure good reconstruction, an event is accepted only if all six nearest neighbors of the water-Cherenkov detector with the highest signal were operational at the time of the event (Pierre Auger Collaboration 2010a). Based on this fiducial cut, any active water-Cherenkov detector with six active neighbors defines an active *elemental cell*. In these conditions, and above the energy at which the detection efficiency saturates, 3 EeV (Pierre Auger Collaboration 2010a), the total exposure of the SD array is 23,520 km² yr sr.

Due to the steepness of the energy spectrum, any mild bias in the estimate of the shower energy with time or zenith angle can lead to significant distortions of the event counting rate above a given energy. It is thus critical to control the energy estimate in searching for anisotropies. The procedure followed to obtain an unbiased estimate of the shower energy consists in correcting measurements of shower signals for the influences of weather effects (Pierre Auger Collaboration 2009) and the geomagnetic field (Pierre Auger Collaboration 2011b). Using the constant intensity cut method (Hersil 1961), the shower signal is then converted to the value that would have been expected had the shower arrived at a zenith angle of 38° . This reference shower signal is finally converted into energy using a calibration curve based on hybrid events measured simultaneously by the SD array and FD telescopes, since the latter can provide a calorimetric measurement of the energy (Pierre Auger Collaboration 2008).

In searching for anisotropies, it is also critical to know accurately the effective time-integrated collecting area for a flux from each direction of the sky, or in other words, the

directional exposure ω of the Observatory. For each elemental cell, this is obtained through the integration over local sidereal time (LST) α^0 of $x^{(i)}(\alpha^0) \times a_{\text{cell}}(\theta) \times \epsilon(\theta, \varphi, E)$, with $x^{(i)}(\alpha^0)$ the total operational time of the cell (i) at LST α^0 , $a_{\text{cell}}(\theta) = 1.95 \cos \theta$ km² the geometric aperture of each elemental cell under incidence zenith angle θ (Pierre Auger Collaboration 2010a), and $\epsilon(\theta, \varphi, E)$ the detection efficiency under incidence zenith angle θ and azimuth angle φ at energy E . In the same way as in Pierre Auger Collaboration (2011a), the small modulation of the exposure in α^0 due to the variations of $x^{(i)}$ can be accounted for by re-weighting the events with the number of elemental cells at the LST of each event k , $\Delta N_{\text{cell}}(\alpha_k^0)$. Since both θ and φ depend only on the difference $\alpha - \alpha^0$, the integration over α^0 can then be substituted for an integration over the hour angle $\alpha' = \alpha - \alpha^0$ so that the directional exposure actually does not depend on right ascension when the $x^{(i)}$ are assumed to be independent of the LST:

$$\omega(\delta, E) = \sum_{i=1}^{n_{\text{cell}}} x^{(i)} \int_0^{24h} d\alpha' \times a_{\text{cell}}(\theta(\alpha', \delta)) \epsilon(\theta(\alpha', \delta), \varphi(\alpha', \delta), E). \quad (1)$$

The zenithal dependence of the detection efficiency $\epsilon(\theta, \varphi, E)$ can be obtained directly from the data in an empirical way (Pierre Auger Collaboration 2012). Additional effects have an impact on ω , such as the azimuthal dependence of the efficiency due to geomagnetic effects, the corrections to both the geometric aperture of each elemental cell and the detection efficiency due to the tilt of the array, and the corrections due to the spatial extension of the array. Accounting for all these effects, the resulting dependence of ω on declination can be found in Pierre Auger Collaboration (2012). For a wide range of declinations between $\simeq -89^{\circ}$ and $\simeq -20^{\circ}$, the directional exposure is $\simeq 2500$ km² yr at 1 EeV, and $\simeq 3500$ km² yr for any energy above full efficiency. Then, at higher declinations, it smoothly falls to zero, with no exposure above 20° declination.

The detection of significant dipole or quadrupole moments above EeV energies would be of considerable interest. Dipole and quadrupole patterns are encoded in the low-order a_{1m} and a_{2m} coefficients of the multipolar expansion of any angular distribution over the sphere $\Phi(\mathbf{n})$:

$$\Phi(\mathbf{n}) = \sum_{\ell \geq 0} \sum_{m=-\ell}^{\ell} a_{\ell m} Y_{\ell m}(\mathbf{n}), \quad (2)$$

where \mathbf{n} denotes a unit vector taken in equatorial coordinates. Due to the non-uniform and incomplete coverage of the sky at the Pierre Auger Observatory, the estimated coefficients $\bar{a}_{\ell m}$ are determined in a two-step procedure. First, from any event set with arrival directions $\{\mathbf{n}_1, \dots, \mathbf{n}_N\}$ recorded at LST $\{\alpha_1^0, \dots, \alpha_N^0\}$, the multipolar coefficients of the angular distribution coupled to the exposure function are estimated through

$$\bar{b}_{\ell m} = \sum_{k=1}^N \frac{Y_{\ell m}(\mathbf{n}_k)}{\Delta N_{\text{cell}}(\alpha_k^0)}. \quad (3)$$

$\Delta N_{\text{cell}}(\alpha_k^0)$ corrects for the slightly non-uniform directional exposure in right ascension. Then, assuming that the multipolar expansion of the angular distribution $\Phi(\mathbf{n})$ is *bounded* to ℓ_{max} , the first $b_{\ell m}$ coefficients with $\ell \leq \ell_{\text{max}}$ are related to the

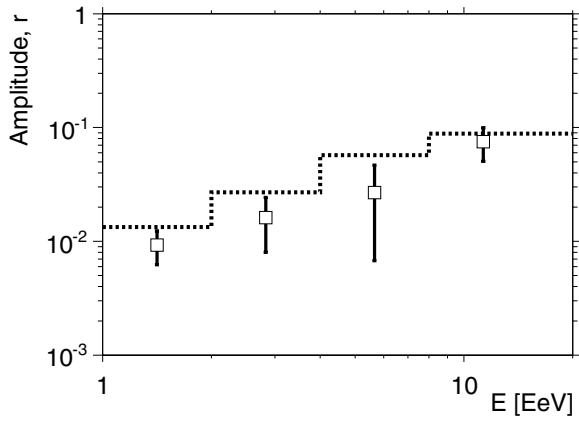


Figure 1. Reconstructed amplitude of the dipole as a function of the energy. The dotted line stands for the 99% CL upper bounds on the amplitudes that would result from fluctuations of an isotropic distribution.

non-vanishing $a_{\ell m}$ through

$$\bar{b}_{\ell m} = \sum_{\ell'=0}^{\ell_{\max}} \sum_{m'=-\ell'}^{\ell'} [K]_{\ell m}^{\ell' m'} \bar{a}_{\ell' m'}, \quad (4)$$

where the matrix K is entirely determined by the directional exposure:

$$[K]_{\ell m}^{\ell' m'} = \int_{\Delta\Omega} d\Omega \omega(\mathbf{n}) Y_{\ell m}(\mathbf{n}) Y_{\ell' m'}(\mathbf{n}). \quad (5)$$

Inverting Equation (4) allows us to recover the underlying $\bar{a}_{\ell m}$, with a resolution proportional to $([K^{-1}]_{\ell m}^{\ell m} \bar{a}_{00})^{0.5}$ (Billoir & Deligny 2008). As a consequence of the incomplete coverage of the sky, this resolution deteriorates by a factor larger than two each time ℓ_{\max} is incremented by 1. With our present statistics, this prevents the recovery of each coefficient with good accuracy as soon as $\ell_{\max} \geq 3$, which is why we restrict ourselves to dipole and quadrupole searches.

We first assume that the angular distribution of cosmic rays is modulated by a *pure* dipole and parameterize the intensity $\Phi(\mathbf{n})$ in any direction as

$$\Phi(\mathbf{n}) = \frac{\Phi_0}{4\pi} (1 + r \mathbf{d} \cdot \mathbf{n}), \quad (6)$$

where \mathbf{d} denotes the dipole unit vector. The dipole pattern is here fully characterized by a declination δ_d , a right ascension α_d , and an amplitude r corresponding to the maximal anisotropy contrast: $r = (\Phi_{\max} - \Phi_{\min}) / (\Phi_{\max} + \Phi_{\min})$. The estimation of these three coefficients is straightforward from the estimated spherical harmonic coefficients $\bar{a}_{\ell m}$. The reconstructed amplitudes \bar{r} are shown in Figure 1 as a function of the energy. The 99% CL upper bounds on the amplitudes that would result from fluctuations of an isotropic distribution are indicated by the dotted line. One can see that within the statistical uncertainties, there is no evidence of any significant signal. In Figure 2, the corresponding directions are shown in orthographic projection with the associated uncertainties, as a function of the energy. Both angles are expected to be randomly distributed in the case of independent samples whose parent distribution is isotropic. It is thus interesting to note that all reconstructed declinations are in the equatorial southern hemisphere, and to note also the intriguing smooth alignment of the phases in right ascension as a function of the energy. In our previous report on first harmonic

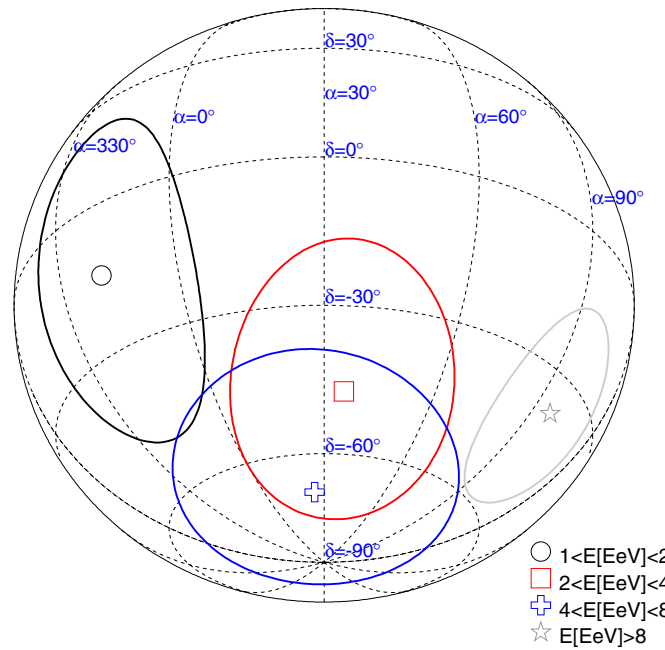


Figure 2. Reconstructed declination and right ascension of the dipole with corresponding uncertainties, as a function of the energy, in orthographic projection.

(A color version of this figure is available in the online journal.)

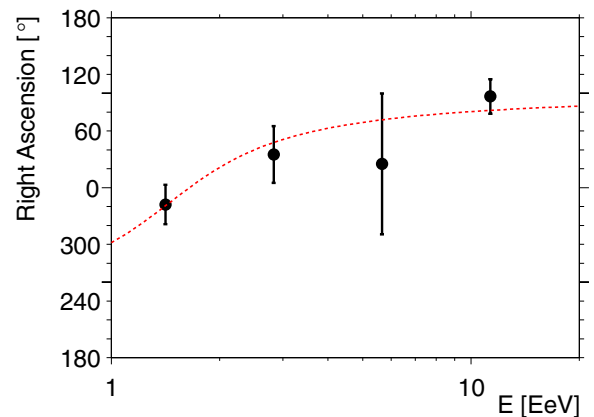


Figure 3. Reconstructed right ascension of the dipole as a function of the energy. The smooth fit to the data of Pierre Auger Collaboration (2011a) is shown as the dashed line (see the text).

(A color version of this figure is available in the online journal.)

analysis in right ascension (Pierre Auger Collaboration 2011a), we already pointed out this alignment, and stressed that such a consistency of phases in adjacent energy intervals is expected with a smaller number of events than the detection of amplitudes standing out significantly above the background noise in the case of a real underlying anisotropy. This motivated us to design a *prescription* aimed at establishing at 99% CL whether this consistency in phases is real, using the exact same analysis as the one reported in Pierre Auger Collaboration (2011a). The prescribed test will end once the total exposure since 2011 June 25 reaches 21,000 km² yr sr. The smooth fit to the data of Pierre Auger Collaboration (2011a) is shown as a dashed line in Figure 3, restricted to the energy range considered here. Though the phase between 4 and 8 EeV is poorly determined due to the corresponding direction in declination pointing close to the equatorial south pole, it is noteworthy that a consistently

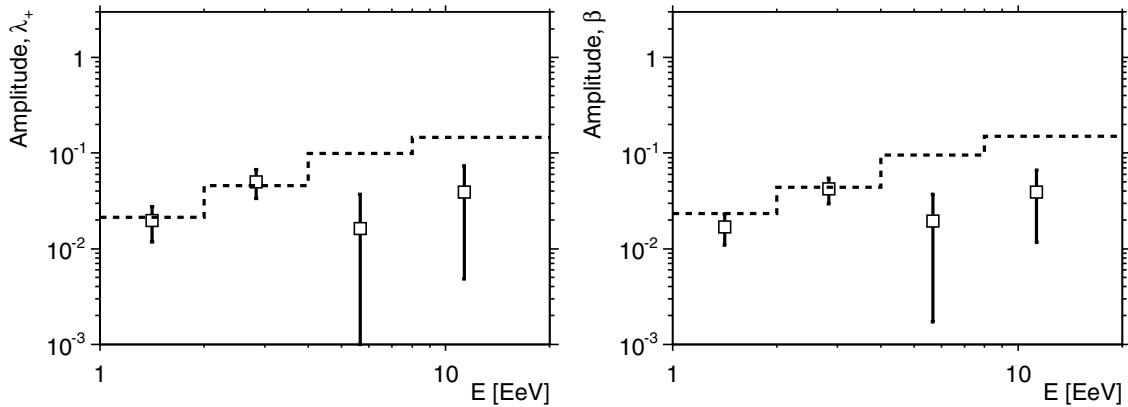


Figure 4. Amplitudes of the quadrupole moment as a function of the energy using a multipolar reconstruction up to $\ell_{\max} = 2$. The dotted lines stand for the 99% CL upper bounds on the amplitudes that could result from fluctuations of an isotropic distribution.

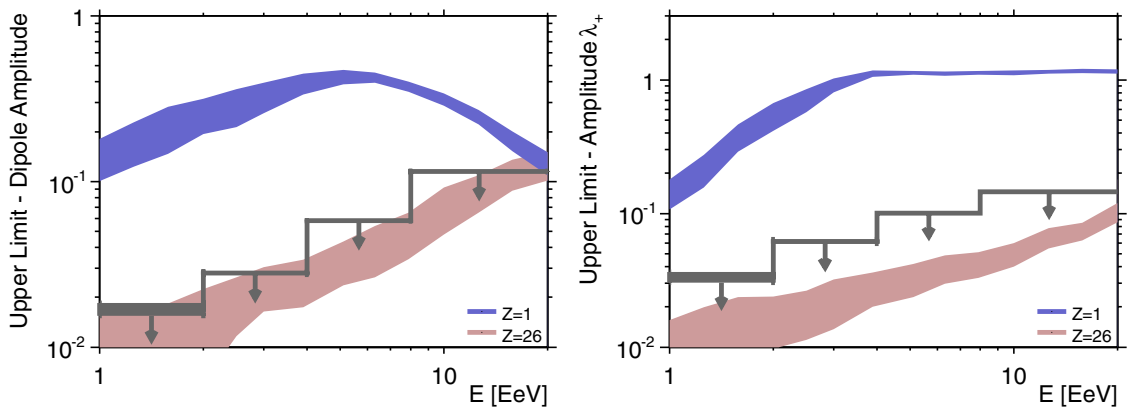


Figure 5. 99% CL upper limits on dipole and quadrupole amplitudes as a function of the energy. Some generic anisotropy expectations from stationary galactic sources distributed in the disk are also shown, for various assumptions on the cosmic ray composition. The fluctuations of the amplitudes due to the stochastic nature of the turbulent component of the magnetic field are sampled from different simulation data sets and are shown by the bands.

(A color version of this figure is available in the online journal.)

smooth behavior is observed using the analysis presented here and applied to a data set containing two additional years of data.

Assuming now that the angular distribution of cosmic rays is modulated by a dipole *and* a quadrupole, the intensity $\Phi(\mathbf{n})$ can be parameterized in any direction \mathbf{n} as

$$\Phi(\mathbf{n}) = \frac{\Phi_0}{4\pi} (1 + r\mathbf{d} \cdot \mathbf{n} + \lambda_+(\mathbf{q}_+ \cdot \mathbf{n})^2 + \lambda_0(\mathbf{q}_0 \cdot \mathbf{n})^2 + \lambda_-(\mathbf{q}_- \cdot \mathbf{n})^2), \quad (7)$$

with the constraint $\lambda_+ + \lambda_- + \lambda_0 = 0$. It is convenient to define the quadrupole amplitude $\beta \equiv (\lambda_+ - \lambda_-)/(2 + \lambda_+ + \lambda_-)$, which provides a measure of the maximal quadrupolar contrast in the absence of a dipole. Hence, any quadrupolar pattern can be fully described by two amplitudes (β, λ_+) and three angles: (δ_+, α_+) , which define the orientation of \mathbf{q}_+ , and (α_-) , which defines the direction of \mathbf{q}_- in the orthogonal plane to \mathbf{q}_+ . The third eigenvector \mathbf{q}_0 is orthogonal to \mathbf{q}_+ and \mathbf{q}_- . The estimated amplitudes $\bar{\lambda}_+$ and $\bar{\beta}$ are shown in Figure 4 as functions of the energy. In the same way as for dipole amplitudes, the 99% CL upper bounds on the quadrupole amplitude that could result from fluctuations of an isotropic distribution are indicated by the dashed lines. Throughout the energy range, there is no evidence for anisotropy.

There are small uncertainties in correcting the estimator of the energy for weather and geomagnetic effects, and these propagate into systematic uncertainties in the measured anisotropy

parameters. As well, anisotropy parameters may be altered in a systematic way by energy dependence of the attenuation curve. All these systematic effects have been quantified (Pierre Auger Collaboration 2012). They do not change significantly the results presented here.

From these analyses, upper limits on dipole and quadrupole amplitudes can be derived at 99% CL. They are shown in Figure 5 for the dipole amplitudes, accounting for the systematic uncertainties. We illustrate now their astrophysical interest by calculating the amplitudes of anisotropy expected in a toy scenario in which sources of EeV-cosmic rays are stationary, densely, and uniformly distributed in the galactic disk, and emit particles in all directions.

Both the strength and the structure of the magnetic field in the Galaxy, known only approximately, play a crucial role in the propagation of cosmic rays. The field is thought to contain a large-scale regular component and a small-scale turbulent one, both having a local strength of a few microgauss (see, e.g., Beck 2001). While the turbulent component dominates in strength by a factor of a few, the regular component imprints dominant drift motions as soon as the Larmor radius of cosmic rays is larger than the maximal scale of the turbulences (thought to be in the range 10–100 pc). We adopt here a recent parameterization of the regular component obtained by fitting model field geometries to Faraday rotation measures of extragalactic

radio sources and polarized synchrotron emission (Bisymmetric Spiral Structure (BSS) model, with anti-symmetric halo with respect to the galactic plane; Pshirkov et al. 2011). In addition to the regular component, a turbulent field is generated according to a Kolmogorov power spectrum and is pre-computed on a three-dimensional grid periodically repeated in space. The size of the grid is selected to match the maximal scale of turbulences (taken here as 100 pc), and the strength of the turbulent component is taken as three times the strength of the regular one. To describe the propagation of cosmic rays with energies $E \geq 1$ EeV in such a magnetic field, the direct integration of trajectories is the most appropriate tool. To obtain the anisotropy of cosmic rays emitted from sources uniformly distributed in a cylinder with a radius of 20 kpc from the galactic center and with a height of ± 100 pc, we adopt a method first proposed in Thielheim & Langhoff (1968). It consists in back-tracking anti-particles with random directions from the Earth to outside the Galaxy. Each test particle *probes* the total luminosity along the path of propagation from each direction as seen from the Earth. For *stationary sources emitting cosmic rays in all directions*, the expected flux in the initial sampled direction is proportional to the time spent by each test particle in the source region.

The amplitudes of anisotropy obviously depend on the rigidity E/Z of the cosmic rays, with Z the electric charge of the particles. Since we only aim at illustrating the upper limits, we consider two extreme single primaries: protons and iron nuclei. The calculation of anisotropy amplitudes for single primaries is useful to probe the allowed contribution of each primary as a function of the energy.

The dipole and quadrupole amplitudes obtained for several energy values covering the range $1 \leq E/\text{EeV} \leq 20$ are shown in Figure 5. To probe unambiguously amplitudes down to the percent level, it is necessary to generate simulated event sets with at least $\simeq 5 \times 10^5$ test particles. Such a number of simulated events allow us to shrink statistical uncertainties on amplitudes at the 0.5% level. Meanwhile, there is an intrinsic variance in the model for each anisotropy parameter due to the stochastic nature of the turbulent component of the magnetic field. This variance is estimated through the simulation of 20 sets of 5×10^5 test particles, where the configuration of the turbulent component is frozen in each set. The rms of the amplitudes sampled in this way is shown by the bands in Figure 5.

The resulting amplitudes for protons largely stand above the allowed limits. Consequently, unless the strength of the magnetic field is much higher than in the picture used here, the upper limits derived in this analysis exclude that the light component of cosmic rays comes from galactic stationary sources densely distributed in the galactic disk and emitting in all directions. To respect the dipole limits below the ankle energy, the fraction of protons should not exceed $\simeq 10\%$ of the cosmic ray composition. This is particularly interesting in the view of the indications for the presence of a light component around 1 EeV from shower depth maximum measurements (Pierre Auger Collaboration 2010b; Abbasi et al. 2010; Jui et al. 2011), though firm interpretations of these measurements in terms of the atomic mass still suffer from some ambiguity due to the uncertain hadronic interaction models used to describe the shower developments. On the other hand, if the cosmic ray composition around 1 EeV results from a mixture containing heavy elements of galactic origin and light elements of extragalactic origin, upper limits can be respected. This is because large-scale anisotropy amplitudes below the percent level

are expected for extragalactic cosmic rays, due to the motion of the Galaxy relative to a possibly stationary extragalactic cosmic ray rest frame (Kachelriess & Serpico 2006; Harari et al. 2010).

Future measurements of composition below 1 EeV will come from the low energy extension HEAT now available at the Pierre Auger Observatory (Mathes et al. 2011). Combining these measurements with large-scale anisotropy ones will then allow us to further understand the origin of cosmic rays at energies less than 4 EeV.

The successful installation, commissioning, and operation of the Pierre Auger Observatory would not have been possible without the strong commitment and effort from the technical and administrative staff in Malargüe.

We are very grateful to the following agencies and organizations for financial support: Comisión Nacional de Energía Atómica, Fundación Antorchas, Gobierno De La Provincia de Mendoza, Municipalidad de Malargüe, NDM Holdings, and Valle Las Leñas, in gratitude for their continuing cooperation over land access, Argentina; the Australian Research Council; Conselho Nacional de Desenvolvimento Científico e Tecnológico (CNPq), Financiadora de Estudos e Projetos (FINEP), Fundação de Amparo à Pesquisa do Estado de Rio de Janeiro (FAPERJ), Fundação de Amparo à Pesquisa do Estado de São Paulo (FAPESP), Ministério de Ciência e Tecnologia (MCT), Brazil; AVCR AV0Z10100502 and AV0Z10100522, GAAV KJB100100904, MSMT-CR LA08016, LG11044, MEB111003, MSM0021620859, LA08015 and TACR TA01010517, Czech Republic; Centre de Calcul IN2P3/CNRS, Centre National de la Recherche Scientifique (CNRS), Conseil Régional Ile-de-France, Département Physique Nucléaire et Corpusculaire (PNC-IN2P3/CNRS), Département Sciences de l'Univers (SDU-INSU/CNRS), France; Bundesministerium für Bildung und Forschung (BMBF), Deutsche Forschungsgemeinschaft (DFG), Finanzministerium Baden-Württemberg, Helmholtz-Gemeinschaft Deutscher Forschungszentren (HGF), Ministerium für Wissenschaft und Forschung, Nordrhein-Westfalen, Ministerium für Wissenschaft, Forschung und Kunst, Baden-Württemberg, Germany; Istituto Nazionale di Fisica Nucleare (INFN), Ministero dell'Istruzione, dell'Università e della Ricerca (MIUR), Italy; Consejo Nacional de Ciencia y Tecnología (CONACYT), Mexico; Ministerie van Onderwijs, Cultuur en Wetenschap, Nederlandse Organisatie voor Wetenschappelijk Onderzoek (NWO), Stichting voor Fundamenteel Onderzoek der Materie (FOM), Netherlands; Ministry of Science and Higher Education, grant Nos. N N202 200239 and N N202 207238, Poland; Portuguese national funds and FEDER funds within COMPETE - Programa Operacional Factores de Competitividade through Fundação para a Ciência e a Tecnologia, Portugal; Romanian Authority for Scientific Research, UEFICDI, Ctr.Nr.1/ASPERA2 ERA-NET, Romania; Ministry for Higher Education, Science, and Technology, Slovenian Research Agency, Slovenia; Comunidad de Madrid, FEDER funds, Ministerio de Ciencia e Innovación and Consolider-Ingenio 2010 (CPAN), Xunta de Galicia, Spain; Science and Technology Facilities Council, United Kingdom; Department of Energy, Contract Nos. DE-AC02-07CH11359, DE-FR02-04ER41300, National Science Foundation, grant No. 0450696, The Grainger Foundation USA; NAFOSTED, Vietnam; Marie Curie-IRSES/EPLANET, European Particle Physics Latin American Network, European Union 7th Framework Program, grant No. PIRSES-2009-GA-246806; and UNESCO.

REFERENCES

- Abbasi, R. U., Abu-Zayyad, T., Al-Seady, M., et al. (The HiRes Collaboration) 2010, [PhRvL](#), **104**, 161101
- Beck, R. 2001, [SSRv](#), **99**, 243
- Berezinsky, V. S., Gazizov, A. Z., & Grigorieva, S. I. 2006, [PhRvD](#), **74**, 043005
- Berezinsky, V. S., Grigorieva, S. I., & Hnatyk, B. I. 2004, [Aph](#), **21**, 617625
- Billoir, P., & Deligny, O. 2008, [JCAP](#), **02**, 009
- Blumenthal, G. R. 1970, [PhRvD](#), **1**, 1596
- Candia, J., Mollerach, S., & Roulet, E. 2003, [JCAP](#), **05**, 003
- Giacinti, G., Kachelrieß, M., Semikoz, D. V., & Sigl, G. 2012, [JCAP](#), **07**, 031
- Harari, D., Mollerach, S., & Roulet, E. 2010, [JCAP](#), **11**, 033
- Hersil, J., Escobar, I., Scott, D., Clark, G., & Olbert, S. 1961, [PhRvL](#), **6**, 22
- Hillas, A. M. 1967, [PhLA](#), **24**, 677
- Jui, C. C. H., et al. (The Telescope Array Collaboration) 2011, Proceedings of the APS Meeting (arXiv:1110.0133)
- Kachelrieß, M., & Serpico, P. 2006, [PhLB](#), **640**, 225
- Mathes, H. J., & (for the Pierre Auger Collaboration) 2011, Proceedings of the 32nd ICRC, (Vol. 3. HE 1.4), 149
- The Pierre Auger Collaboration 2008, [PhRvL](#), **101**, 061101
- The Pierre Auger Collaboration 2009, [Aph](#), **32**, 89
- The Pierre Auger Collaboration 2010a, [NIMPA](#), **613**, 29
- The Pierre Auger Collaboration 2010b, [PhRvL](#), **104**, 091101
- The Pierre Auger Collaboration 2011a, [Aph](#), **34**, 627
- The Pierre Auger Collaboration 2011b, [JCAP](#), **11**, 022
- The Pierre Auger Collaboration 2012, [ApJS](#), **203**, 34
- Pshirkov, M. S., Tinyakov, P. G., Kronberg, P. P., & Newton-McGee, K. J. 2011, [ApJ](#), **738**, 192
- Ptuskin, V., Rogovaya, S. I., Zirakashvili, V. N., et al. 1993, [A&A](#), **268**, 726
- Thielheim, K. O., & Langhoff, W. 1968, [JPhA](#), **1**, 694